ELSEVIER

Biochimica et Biophysica Acta 1274 (1996) 21–30

BBA Biochimica et Biophysica Acta

Functional organization of the photosynthetic apparatus of the primitive alga *Mantoniella squamata*

Birgit Hecks [a], Christian Wilhelm [b], Hans-Wilhelm Trissl [a,*]

[a] *Abt. Biophysik, Fachbereich Biologie / Chemie, Universität Osnabrück, Barbarastraße 11, D-49069 Osnabrück, Germany*
[b] *Botanisches Institut, Universität Leipzig, Johannisallee 19-21, D-04031 Leipzig, Germany*

Received 10 August 1995; revised 14 December 1995; accepted 3 January 1996

Abstract

The organization of photosystem I (PS I) and photosystem II (PS II) as well as their light harvesting complexes (LHC) in the thylakoid membrane of *Mantoniella squamata* was characterized by measurements of fluorescence induction and picosecond fluorescence decay kinetics. This microalga possesses a homogeneous thylakoid membrane system for which no state transitions are known and in which the two photosystems are somehow mingled. Here we addressed the questions whether PS I and PS II are in such a close contact that PS I drains excitation energy from PS II as suggested by Trissl and Wilhelm (Trissl, H.-W. and Wilhelm, C. (1993) Trends Biochem. Sci. 18, 415–419) and whether the PS II units themselves are excitonically coupled (connected units) or organized as separated units. By quantitative analysis of fluorescence induction curves we determined the antenna size of PS II to be $N \approx 510$ (all chlorophylls). From the ratio of maximal $F_m/F_o = 3.1$ we conclude that the excitonic contact between PS II and PS I is weak. However, there is significant contact between PS II units as obvious from the sigmoidicity of the fluorescence induction curve. The fluorescence induction kinetics are well described by the connected units model (Lavergne, J. and Trissl, H.-W. (1995) Biophys. J. 65, 2474–2492) using only PS II_α-centers. These results indicate that essentially one population of PS II units (PS II_α) exists in the thylakoid membrane of *Mantoniella* and that the PS II units are in closer contact to each other than to PS I. This closer excitonic contact of PS II units is consistent with the idea of a PS II dimer organization.

Keywords: Antenna organization; Antenna size; Fluorescence measurement

1. Introduction

The prasinophycean algae *Mantoniella squamata* (Chlorophyta) is thought to represent a phylogenetical old relict that has survived in the deep ocean. Its photosynthetic apparatus features several unique properties that render it different from other oxygen-evolving organisms. Although the thylakoid membranes appear to be multilayered, there are no appressed regions that correspond to grana in higher plants and green algae [1]. A peculiarity of the antenna system of *Mantoniella* is therefore its lateral homogeneity, that may lead to a scrambled arrangement of PS I and PS II. Consistent with the lack of structural differentiation of the thylakoid membrane is the absence of state transitions [2]. In higher plants the state transition of the photosynthetic apparatus is thought to be initiated by phosphorylation and dephosphorylation of LHC II in order to adopt the linear electron transport chain to the actual environmental light conditions [3,4].

The inability of *Mantoniella* thylakoids to form grana may be traceable to its unique LHC_{a+b+c} that binds besides chlorophyll *a* (Chl *a*) and Chl *b* also Chl *c*. Although, the LHC_{a+b+c} from *Mantoniella* shows many similarities to the LHC II_{a+b} of higher plants, the N-terminus of LHC_{a+b+c} is shorter by a sequence of 30 amino acids compared to LHC II_{a+b} [5,6]. The absent segment contains a phosphorylation site and is believed to be responsible for stacking and grana formation in higher plants [7]. Hence, the missing segment in *Mantoniella* LHC_{a+b+c} is likely to be the reason for the absence of

Abbreviations: Chl *a*, *b*, *c* chlorophyll *a*, *b*, *c*; DCBQ 2,5-dichlorobenzoquinone; DCMU 3-(3,4-dichlorophenyl)-1,1-dimethylurea; DAD 2,3,5,6-tetramethyl-*p*-phenylenediamine; LHC light harvesting complex; PS I, II photosystem I, II; PSU photosynthetic unit; P680 primary donor of PS II; P700 primary donor of PS I; RC reaction center; RP radical pair.

* Corresponding author. Fax: +49 541 9692870; e-mail: trissl@sfb-bio1.biologie.uni-osnabrueck.de.

PII S0005-2728(96)00005-9

state transitions and grana. Even if the peripheral light harvesting complex of *Mantoniella squamata* and that from *Micromonas pusilla* (Prasinophyceae) [8] combines properties of that of the Chlorophytes and Chromophytes [9], recent investigations indicate a more likely relationship to the LHC II_{a+b} of Chlorophytes rather than to the LHC_{a+c} of Chromophytes [5,6].

The low temperature fluorescence spectrum of *Mantoniella* does not exhibit a PS I-typical emission peak in the range of 720 nm and 735 nm [2,10–12]. This indicates the absence of long-wavelength absorbing pigments. The absent long-wavelength fluorescence emission distinguishes the antenna system of *Mantoniella* from that of other algae and higher plants in which these emission bands are typically found [13–16]. The reason for this may be related to the presence of a uniform type of LHC_{a+b+c} in the thylakoid [11] that serves PS I as well as PS II as a supply for excitons. Such a LHC_{a+b+c} common to both photosystems can be expected to have no long-wavelength absorbing pigments. If the LHC_{a+b+c} would contain them this would drastically diminish the trapping efficiency in the slow FS II, but not in the fast PS I [17].

Recently, it has been pointed out that nature had to avoid the excitonic contact between PS I and PS II because otherwise PS I would drain excitation energy off from PS II [18]. The argument was based on the higher speed of exciton conversion into chemical free energy by PS I in comparison to PS II. Examples for different realizations of the concept to keep the two photosystems apart are the expulsion of PS II into grana (higher plants and most green algae) or the collection of PS II beneath phycobilisomes (cyanobacteria) [19,20]. It is therefore of particular interest to investigate whether or not a separation of both photosystems in *Mantoniella* thylakoids is given. As speculated by two of the authors, *Mantoniella* could be an example for a species that has not invented the segregation yet [18]. Support for this idea came from the low F_m/F_o ratio of approx. 1.4 [21], which indicates strong loss processes in PS II (e.g., by PS I) as well as from the high PS II/PS I ratio of 3 to 4 [2] that is predicted from maintaining a balanced electron flow between PS II and PS I when PS II is operating inefficiently due to PS I quenching. In Fig. 1a a topological scheme is illustrated in which the photosynthetic units (PSU) of PS I and PS II are homogenously embedded in the thylakoid membrane allowing for a variable extent of excitonic contact between all PSUs (connected units). In the present work the term PSU will be defined as the stoichiometric ratio of antenna pigments to RCs of a particular photosystem type (PS I or PS II).

In the present study we find a much higher F_m/F_o ratio than reported in the literature and this fact raises questions on the model shown in Fig. 1a, since a high F_m/F_o value is incompatible with a strongly quenched PS II. Therefore, we inspect two other models. First, all PSUs are arranged as separate packages (Fig. 1b). Second, PS II units are arranged as perfectly coupled dimers and PS I units as well as the dimers are separated (Fig. 1c). Evidence for the latter antenna organization comes from single-particle image-averaging analysis of PS II complexes isolated from the thermophilic cyanobacterium *Synechococcus elongatus* and also from spinach. In both in vitro systems a dimeric aggregation of PS II units was demonstrated [22] and the existence of such dimers in vivo was suggested by several authors [22–27]. It is the aim of this study to find out which of the proposed models of the antenna organization is best suited to describe the thylakoid membranes of *Mantoniella*.

Another aim concerns the extent of heterogeneity of PS II. As mentioned the thylakoid system of *Mantoniella* is not partitioned into grana and stroma regions. This structural differentiation in thylakoids of higher plants is believed to cause one type of heterogeneity of PS II, namely PS II_α in grana membranes and PS II_β in stroma exposed membranes [28]; for review see Refs. [29]. If this is true,

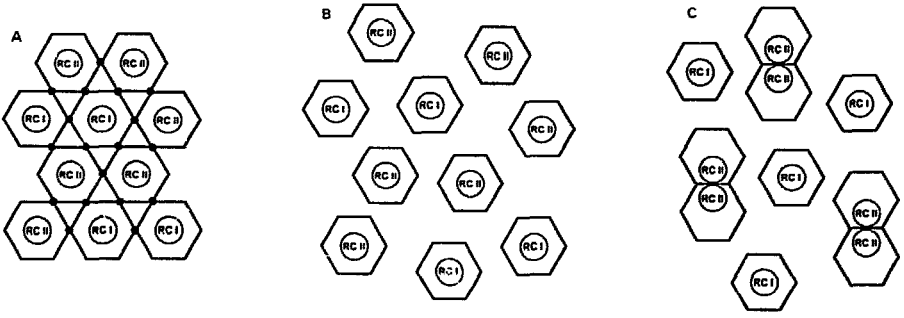

Fig. 1. Models for possible antenna organizations of *Mantoniella* thylakoid membranes with regard to PS I and PS II. The core complexes of PS I and PS II (encircled) are surrounded by the same LHC_{a+b+c} forming the PSUs (hexagons). (a) **Connected units**: All PSUs have excitonic contact at 6 hypothetic sites. (b) **Separate units**: The PSUs without excitonic contact. (c) **Dimer model**: The core complexes of PS II and the surrounding LHC_{a+b+c} form an excitonically well-coupled dimer. The dimers and the PS I units are excitonically separated from each other.

one would not expect this type of heterogeneity in the homogeneous thylakoid membrane system of *Mantoniella*.

2. Materials and methods

Theoretical background. In the present study we utilize recently derived expressions for the fluorescence and photochemical yields as they follow from the exciton-radical pair equilibrium model to fit fluorescence induction curves [30]. In a slightly simplified version this model can be summarized as follows:

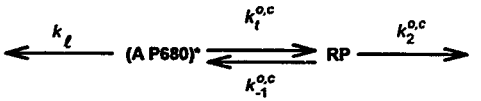

The excited state (A P680)* of the antenna pigments, A, and the primary donor of PS II, P680, can be deactivated by photochemistry in reaction centers (RCs) which may be either in the open (o) or closed state (c) by the formation of the radical pair, RP, with the rate constants, $k_t^{o,c}$, or non-photochemically by loss processes in the antenna system, k_f. The latter include the radiative decay of an antenna pigment (k_{rad}) and, if occasion arises, quenching by PS I. The RP has either the possibility to back-react to the excited state with the rate constants, $k_{-1}^{o,c}$, or to decay in open RCs by the charge stabilization and in closed RCs by non-radiative processes with the rate constants, $k_2^{o,c}$, respectively. For fluorescence induction the molecular rate constants due to RC deactivation can be lumped together in apparent rate constants for open and closed RCs, k_o and k_c:

$$k_o = \frac{k_t^o \cdot k_2^o}{k_{-1}^c + k_2^c}. \tag{1a}$$

$$k_c = \frac{k_t^c \cdot k_2^c}{k_{-1}^c + k_2^c}. \tag{1b}$$

For the present analysis it suffices to relate the fluorescence yield for all open RCs, Φ_o, the fluorescence yield for all closed RCs, Φ_m, and the photochemical yield for all open RCs, $\Phi_p(1)$ with k_o and k_c. The fraction of open RCs is expressed by q ($0 \le q \le 1$). According to Lavergne and Trissl [30], one obtains:

$$\Phi_o = \frac{k_{rad}}{k_o + k_f}, \tag{2a}$$

$$\Phi_m = \frac{k_{rad}}{k_c + k_f}, \tag{2b}$$

$$\Phi_p(1) = \frac{k_o}{k_o + k_f}. \tag{2c}$$

To account for the extent of exciton transfer between PSUs, we assume the following reaction scheme (**connected units model**):

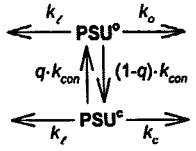

If thermal equilibration of the excited state prior to the primary charge separation within a PSU is presumed and structural details of the contact sites are neglected the inter-unit exciton transfer is described by a single rate constant, k_{con}. Then the sigmoidicity parameter, J [30], reads:

$$J = \left(\frac{\Phi_m}{\Phi_o} - 1\right) \cdot \left(\frac{k_{con}}{k_{con} + k_o + k_f}\right). \tag{3}$$

In order to compare photosynthetic systems with different antenna sizes, N, we introduce intrinsic rate constants for radical pair formation that apply to the naked RC with oxidized and reduced acceptor, respectively:

$$k_{o,c}^{int} = N \cdot k_{o,c} \tag{4}$$

These two intrinsic rate constants may be assumed to be the same in PS II of different organisms. Eq. 4 is valid only for perfect equilibration which was shown to represent an adequate approximation in PS II [31]. One obtains for the extreme fluorescence levels:

$$\Phi_o(N) = \frac{N \cdot k_{rad}}{k_o^{int} + N \cdot k_f}, \tag{5a}$$

$$\Phi_m(N) = \frac{N \cdot k_{rad}}{k_c^{int} + N \cdot k_f}, \tag{5b}$$

for the photochemical quantum yield at $q = 1$:

$$\Phi_p(N) = \frac{k_o^{int}}{k_c^{int} + N \cdot k_f}, \tag{5c}$$

and for the ratio of the extreme fluorescence levels:

$$\frac{\Phi_m(N)}{\Phi_o(N)} = \frac{k_o^{int} + N \cdot k_f}{k_c^{int} + N \cdot k_f}. \tag{5d}$$

Then, theoretical fluorescence induction curves can be calculated from:

$$\Phi_f(q) = \frac{\Phi_m - q \cdot [\Phi_m - \Phi_o \cdot (1 + J)]}{1 + J \cdot q}. \tag{6}$$

and the kinetic law,

$$t = \frac{J \cdot (1-q) - \ln q}{I \cdot \Phi_p(1) \cdot (1+J)}. \quad (7)$$

The sigmoidicity of these fluorescence induction curves is solely determined by the parameter J (sigmoidicity parameter). I stands for the rate of exciton creation per photosynthetic unit. Because a PSU is defined as the stoichiometric ratio of antenna pigments to PS II reaction centers,

$$I = N \cdot \sigma \cdot Q \quad (8)$$

in which N denotes the antenna size (number of isoenergetic antenna pigments per RC), σ the absorption cross-section of these antenna pigments at the excitation wavelength, and Q the photon flux ($cm^{-2} \cdot s^{-1}$) falling onto the sample (optically thin).

In addition to the connected units model where all PSUs are (more or less) connected and the inter-unit exciton exchange is described by a single macroscopic rate constant, k_{conn}, an alternative model was applied to fit the fluorescences induction curves, namely a domain theory. In the present work we took the formalism derived by Den Hollander et al. [32]. The basis of it is that within a domain which is defined by the number of PSUs (domain size, λ) perfect exciton transfer is assumed and between different domains no exciton transfer at all. Theoretical fluorescence induction curves can be calculated with the same apparent rate constants, k_n, k_c, and k_f, introduced for the connected units model. It is worthy of note that, although both theories give fluorescence induction curves that are identical at the extremes of antenna organization, i.e., separate units and lake, at intermediate cases the shapes of the curves due to the different theories are not superimposable [33].

Cell culture. Mantoniella squamata cells were grown under low light conditions ($2\ W \cdot m^{-2}$) in an artificial sea water medium according to Müller [34]. The cells were harvested in the late exponential growth phase by centrifugation at $800 \times g$ onto an agar gel to prevent cell damage that would result in low F_m/F_o values < 1.4. Chl a and Chl b concentrations were determined according to Porra et al. [35]. Absorption spectra were recorded with an Aminco DW-2000 spectrophotometer. The quantitative determination of Chl a in the cells and their absorption spectra yielded an apparent molar absorption coefficient in the Q_y-band of 60 330 $M^{-1} \cdot cm^{-1}$ in *Mantoniella* thylakoids. At the excitation wavelength of 675.5 nm the absorption cross section of a mean Chl a pigment is then $\sigma = 22.5 \cdot 10^{-17}\ cm^2$.

P700 measurements. The concentration of the primary donor of PS I, P700, was calculated from the amplitude of the absorption change at $\lambda = 700.0 \pm 3.5$ nm caused by saturating flashes using a differential absorption coefficient of $\Delta\epsilon = 64\ mM^{-1} \cdot cm^{-1}$ [36]. To reduce scattering the measurements were carried out with cells broken by sonification. The re-reduction was controlled by 2 μM PMS and 5 mM ascorbate. The rereduction kinetics could be well fitted with two phases. The fast phase was clearly separated from the fluorescence transient. The resulting Chl a/P700 ratio was 610 for *Mantoniella* thylakoids and 425 in the case of pea thylakoids.

Fluorescence measurements. Fluorescence induction measurements were performed with a self-built apparatus, that consisted of an electronically switched and stabilized monomode laserdiode emitting at 675.5 nm. Care was taken that the measuring volume of $(1 \cdot 1 \cdot 1)\ cm^3$ was homogeneously illuminated. The intensity was typically 500 $\mu W \cdot cm^{-2}$ corresponding to a photon flux of $1.70 \cdot 10^{15}\ cm^{-2} \cdot s^{-1}$. The photon flux was measured with a calibrated radiometer (Model 110, Centronix, UK). Alternatively, excitation was carried out with a slide projector equipped with a mechanic shutter and a broad band interference filter ($530 < \lambda < 570$ nm). This set-up delivered a photon flux of $2.16 \cdot 10^{15}\ cm^{-2} \cdot s^{-1}$. Fluorescence light was collected under 90° through a broad-band interference filter with steep edges at 683 nm and 718 nm (Dr. H. Anders, Nabburg, Germany). The detector was a large area avalanche photodiode (Advanced Photonix Inc., USA).

In the case of excitation at $\lambda = 675.5$ nm experimentally measured fluorescence intensities, F, are proportional to the apparatus sensitivity, A, the Chl a concentration, [Chl a], and the fluorescence yields, Φ_f (Eq. 6):

$$F = A \cdot [Chl\,a] \cdot \Phi_f. \quad (9a)$$

and for a two-fold heterogeneous system with different antenna sizes and different stoichiometries, e.g., PS I and PS II:

$$F = A \cdot [Chl\,a] \cdot \left(\frac{N_a^{PS1} \cdot \Phi^{PS1} + (PSII/PSI) \cdot N_a^{PSII} \cdot \Phi_{o,m}^{PSII}}{N_a^{PSI} + (PSII/PSI) \cdot N_a^{PSII}} \right). \quad (9b)$$

The relations are useful for a quantitative comparison of different organisms with different pigment compositions. When convenient, the fluorescence intensities were normalized to F_o-values.

Measurements of the fluorescence decay kinetics in the picosecond time range were performed with a set-up described before [37] and the data were analyzed as described elsewhere [38]. The relative initial amplitude follows directly from the expression in the brackets of Eq. 9b:

$$F \propto a_1 \cdot \Phi^{PS1} + a_2 \cdot \Phi^{PSII}. \quad (9c)$$

3. Results

Fluorescence induction measurements were carried out with whole cells of *Mantoniella* at the excitation wave-

lengths $\lambda = 675.5$ nm and $\lambda = 550 \pm 20$ nm (Fig. 2). The curves were not superimposable. The two wavelengths were used to extract different information. Excitation in the green excites chlorophyll at an absorption minimum and leads to minimal light gradients within the cells. These data are used to determine the connectivity between the PSUs assayed by the sigmoidicity parameter, *J*. Narrow band excitation at 675.5 nm excites virtually only Chl *a* in its Q_y-band. However, at this wavelength cell internal light-gradients distort the shape of the fluorescence rise. These latter data were used to determine the Chl *a* antenna size and to quantify fluorescence yields normalized to the Chl *a* concentration. The latter two pieces of information can be obtained solely at an excitation wavelength where only one antenna pigment type absorbs. At $\lambda = 675.5$ nm this is given because the absorption of Chl *b* and Chl *c* is negligible.

Fluorescence induction at 675.5 nm. In order to quantify the results from *Mantoniella* to the greatest extent possible and to assess the rate constant for losses in the antenna system, k_f, we related our data to stacked thylakoids from *Pisum sativum*, that were investigated in parallel experiments but are not further described here. For the latter system the exciton-radical pair equilibrium model is well established and the rate constants are known with sufficient accuracy [39–41]. Both systems show the same shape of the fluorescence emission spectra. Compared to pea thylakoids the *Mantoniella* spectrum is 1.5 nm blue-shifted, which causes a 16% less detectable fluorescence yield of *Mantoniella* compared to peas due to the smaller spectral overlap between the fluorescence spectrum and the transmission spectrum of the bandpass filter in the emission light path (data not shown).

The analysis of the fluorescence induction kinetics obtained by excitation at 675.5 nm (Fig. 2) yielded a Chl *a* antenna size of $N = 287 \pm 22$ for PS II of *Mantoniella*. In comparison, our pea thylakoids showed a Chl *a* antenna size of $N = 172 \pm 11$.

Fluorescence induction at 550 nm. A fluorescence induction curve normalized to F_o of DCMU-poised whole

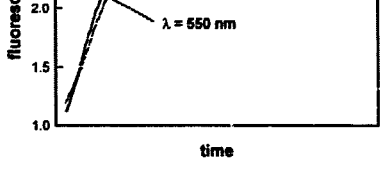

Fig. 2. Comparison of the fluorescence induction curves resulting by excitation at 675.5 nm and 550 nm. The abscissa of both induction curves were adjusted to achieve optimal overlap of the curves.

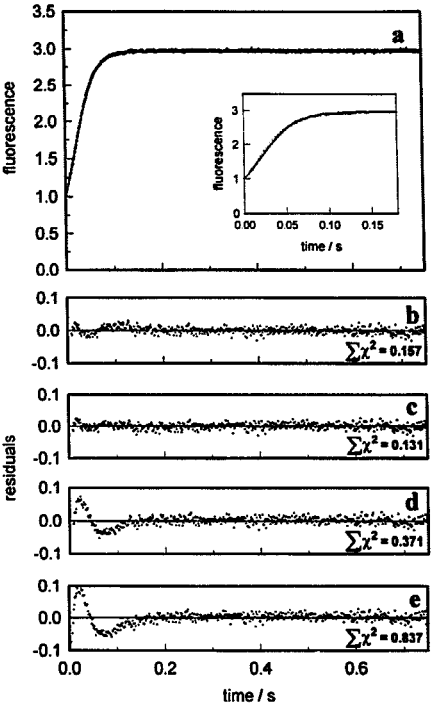

Fig. 3. (a) Fluorescence induction curve (dots) from intact cells of *Mantoniella squamata* in the presence of 200 μM ferricyanide, 10 μM DAD and 20 μM DCMU (the latter was added in the dark) on a time scale of 0 to 700 ms. The Chl *a* concentration was to 2 μM. The curve was first normalized to the true F_o and then 6% fluorescence due to PS I was subtracted. Inset: The same curve on a time scale 0 to 180 ms. Note, that the curves start from an increased F'_o-level. The data were fitted under four different assumptions. **Connected units model:** The theoretical curve (solid line in a and inset) was calculated by using Eqs. 6 and 7 with the three best fit parameters, F_m / F_o (3.0), J (0.89), and $I \cdot \Phi_p(1)$. The corresponding residuals are shown in b. **Connected units model with heterogeneity:** Here we allowed for PS II_β (assumptions: separated units and $F^{\beta}_{o,m} = F^{\alpha}_{o,m}$) in addition to PS II_α (connected units). The ratio of antenna sizes N_α / N_β was 2 and PS II_β amounted to 10% of PS $II_{\alpha+\beta}$ (residuals in c). **Dimer model:** The theoretical curve was calculated with the equations derived for domains [32]. Residuals of the best fit for dimers are shown in d. **Separate units model:** Residuals of the best fit for the (domain size) = 1 using the two fit parameters, F_m / F_o and $I \cdot \Phi_p(1)$, are displayed in e. The corresponding theoretical curve is shown in a (inset, dashed line). The parameters used for all fits were: $k_f = (1.75\ \text{ns})^{-1}$, $k_n = (0.561\ \text{ns})^{-1}$, and $k_c = (4.690\ \text{ns})^{-1}$.

cells of *Mantoniella squamata* upon 550 nm excitation is shown in Fig. 3a (points). The curve starts at an increased F'_o level. The true F_o value (PS I and PS II) was determined from separate measurements (without DCMU) with either 200 μM ferricyanide + 10 μM DAD, or 1 μM DCBQ, or dark-adaptation without any additions. All three values agreed within the experimental error of 5%. It was checked that neither DAD nor DCBQ at concentration

used in experiments quenched the excited state at the concentrations employed. The increased F_o' level followed after DCMU addition can be explained by a back-transfer of electrons from the semiquinone of Q_B to Q_A [30,42]. It was not possible to get the true F_o value in the presence of DCMU although ferricyanide and DAD where added before. A possible reason for the incomplete reoxidation of the semiquinone may be the limited access of DAD to the Q_B-binding site.

The curve shown in Fig. 3a was corrected for a the PS I fluorescence contribution of 6% relative to F_o (see below). The resulting high value of F_m/F_o of 3 indicates that PS II is not strongly quenched by PS I.

The induction curve in Fig. 3a displays a marked sigmoidicity that is indicative of PS II connectivity (inset; compare deviations to the dashed line). A fit of the data with Eqs. 6 and 7 **(connected units)** is shown in Fig. 3a by a solid line. The corresponding residuals are displayed in Fig. 3b. The best fit yielded a sigmoidicity parameter of $J = 0.89$. Notably, the sum over the squared residuals decreased only insignificantly when allowing for a PS II heterogeneity, i.e., for α-centers and β-centers (Fig. 3c).

Another fit of the fluorescence induction curve was carried out using the domain theory of Den Hollander et al. [32]. The residuals for the case of dimers (domain size = 2) is shown in Fig. 3d. Attempts to analyze the curve with larger domain sizes lead to better fits with nearly comparable fit quality of Fig. 3c for a domain size of 4 (not shown). Applying the extreme case of separate units (domain size = 1) yielded the worst residuals for the best fit (Fig. 3e). The corresponding theoretical curve is shown in Fig. 3a (inset, dashed line) to demonstrate the sigmoidicity present in the experimental fluorescence induction curve.

Time-resolved fluorescence decay. The fluorescence decay kinetics of whole cells of *Mantoniella* were measured under F_o- and F_m-conditions on different time bases (Fig. 4a and b, respectively). The curves were analyzed by five parameter fits, three parameters belonging to the exciton-radical pair equilibrium model of PS II ($k_t^{o,c}$, $k_{-1o,c}$, $k_2^{o,c}$) and two parameters belonging to PS I: the relative amplitude of PS I fluorescence, a_1, and one rate constant for the exciton decay of PS I, $k_t^{PS\ I}$. The simultaneous fit of the traces in Fig. 4 yielded the parameters listed in the figure legend. The molecular rate constants of open and closed RCs can be combined to the apparent rate constants, $k_o = (0.561\ \text{ns})^{-1}$ and $k_c = (5.074\ \text{ns})^{-1}$ according to Eq. 1. The fits were obtained with a rate constant for losses of $k_l = (1.75\ \text{ns})^{-1}$. This value resulted from the global analysis outlined in the discussion.

The stoichiometric ratio of PS II/PS I calculated from the ratio of the relative initial fluorescence amplitudes due to PS I and PS II, $a_2/a_1 = 2.07$ according to Eq. 11 (see Section 4) was PS II/PS I ≈ 1.43. Furthermore, the fluorescence yields can be calculated from the rate constants to be $\Phi^{PS\ I} = 0.0031$ and $\Phi_o^{PS\ II} = 0.0236$. Taking the stoichometric ratio of 1.43 and the antenna sizes of PS II, N_a^{PS}

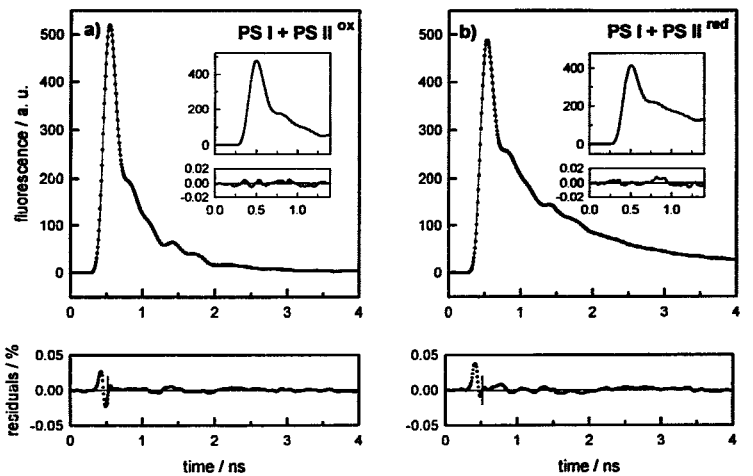

Fig. 4. Fluorescence decay kinetics from intact cells of *Mantoniella squamata* performed with 30 ps laser flashes at 532 nm. (a) F_o-condition (1 mM ferricyanide +50 μM DAD). Top: Fluorescence decay kinetics on a slow (500 ps/div) and fast time scale (200 ps/div; inset). Fit parameter for PS II: $k_t^o = (0.481\ \text{ns})^{-1}$, $k_{-1}^o = (2.504\ \text{ns})^{-1}$, $k_2^o = (0.419\ \text{ns})^{-1}$, fixed parameter: $k_l = (1.75\ \text{ns})^{-1}$. Fit parameters for PS I: $k_t^{PS\ I} = (0.066\ \text{ns})^{-1}$, relative fluorescence amplitude ratio of PS I and PS II, $a_2/a_1 = 2.16$. Fixed parameter: $k_l = (1.75\ \text{ns})^{-1}$. Bottom: Residuals of the best fit (the bar indicates the start of this particular fit). (b) F_m-conditions (100 μM DCMU, preillumiation for 200 ms with broadband interference filter (530 nm < λ < 570 nm, 2 mW · cm^{-2}). Top: Fluorescence decay kinetics on a slow (500 ps/div) and fast time scale (200 ps/div; inset). Fit parameter for PS II: $k_t^c = (1.965\ \text{ns})^{-1}$, $k_{-1}^c = (0.723\ \text{ns})^{-1}$, $k_2^c = (1.144\ \text{ns})^{-1}$, fixed parameters: $k_l = (1.75\ \text{ns})^{-1}$. Fit parameters for PS I: $k_t^{PS\ I} = (0.060\ \text{ns})^{-1}$, relative fluorescence amplitude ratio of PS I and PS II, $a_2/a_1 = 1.87$. Fixed parameter: $k_l = (1.75\ \text{ns})^{-1}$. Bottom: Residuals of the best fit.

$n = 287$ and PS I, $N_a^{PS\,I} = 200$ (see discussion), according to Eq. 9b this yields a 6% PS I contribution on F_o (subtracted in the fluorescence induction curve in Fig. 3).

4. Discussion

Antenna size. The analysis of the fluorescence yield rise of DCMU-poised membranes under dc-light has been applied before to estimate the absorption cross section of PSUs [43,44]. In the present study we estimated the absolute antenna size (e.g., stoichiometric ratio of functionally coupled antenna pigments to a RC) using a theory of fluorescence induction, that includes a time axis scaled in hits per s and PSU (Eqs. 6 to 8). In the case of 675.5 nm excitation Eq. 8 can be solved for the antenna size, N, since I was given by the best fit, the quantum flux Q was directly measured, and the absorption cross section σ was determined as described in Section 2. At this wavelength direct excitation of Chl *b* and Chl *c* is negligible. Furthermore, energy up-hill transfer from excited Chl *a* to Chl *b* or Chl *c* is also negligible, since the Boltzmann equilibrium for the excited state lies almost completely on Chl *a*. Therefore, one can approximate N in Eq. 8 with the number of Chl *a* molecules connected to a RC, N_a.

The fits of many fluorescence induction curves obtained with different cell cultures (all grown at 2 $W \cdot m^{-2}$) yielded a mean Chl *a* antenna size of $N_a = 287 \pm 22$. Taking the Chl *a*/Chl *b* ratio of 1.5 and Chl *a*/Chl *c* ratio of 8.6 [11] found as the average in *Mantoniella* thylakoids, one obtains a total chlorophyll antenna size of PS II in *Mantoniella* of approx. $N_{a+b+c} = 511$. This is by a factor about 2 larger than the PS II antenna size typically found in chloroplasts of higher plants, i.e., our peas grown at light intensities of 20 $W \cdot m^{-2}$ ($N_{a+b} \simeq 245$, Chl *a*/Chl *b* = 2.3).

To calculate the stoichiometric ratio of PS II/PS I one needs a further defining equation which is given by stoichiometric relations in the sample:

$$[Chl\,a] = \frac{PS\,II}{PS\,I} \cdot [P700] \cdot N_a^{PS\,II} + [P700] \cdot N_a^{PS\,I}. \quad (10)$$

Solving Eqs. 9b,c and 10 for PS II/PS I yields:

$$\frac{PS\,II}{PS\,I} = \frac{(a_2/a_1) \cdot (Chla/P700)}{(a_2/a_1 + 1) \cdot N_a^{PS\,II}}. \quad (11)$$

This equation was derived for the special case of exciting Chl *a* only. However, the time resolved fluorescence measurements were carried out at $\lambda = 532$ nm were all chlorophylls absorbed. In our data evaluation this excitation difference was not taking into account, since differences in the pigment composition between both photosystems are not known with certainty and possible differences can be estimated to be very small because only one type of peripheral LHC has been found [11]. Furthermore, if equal Chl *a*/Chl *b* and Chl *a*/Chl *c* ratios for both photosystems are assumed a corresponding factor would cancel in Eq. 11.

The PS II/PS I ratio in *Mantoniella* thylakoids yields 1.43 as derived from the initial fluorescence amplitudes. Together with the stoichiometric ratio of PS II/PS I of 1.43 and the Chl *a*/P700 ratio of 610 for *Mantoniella* the Chl *a* antenna size of PS I follows from Eq. 10 to be about $N_a^{PS\,I} = 200$ resulting in the total antenna size of $N_{a+b+c}^{PS\,I} = 355$.

In the case of pea thylakoids the calculation of the antenna size of the PS I is more complex. First the (PS II_α + PS II_β)/PS I ratio was calculated according to Eq. 11, extended by PS II_α and PS II_β terms and on the basis of Chl *a* + *b* data. To get the Chl *a* + *b* antenna size of PS II_α, we used the determined Chl *a* antenna size from

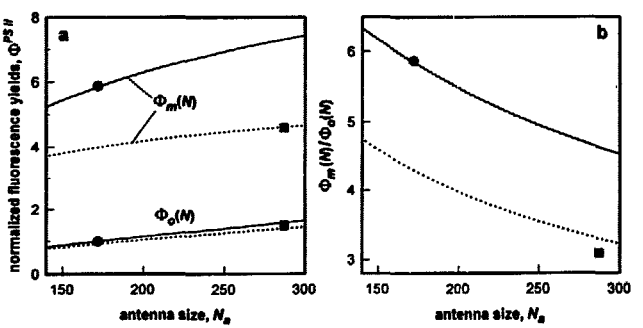

Fig. 5. (a) Dependence of $\Phi_o^{PS\,II}$ and $\Phi_m^{PS\,II}$ on the antenna size for two rate constants for antenna losses as indicated assuming identical properties of the PS II reaction centers calculated by Eqs. 5a and b. Experimental values for pea thylakoids (●) and *Mantoniella* (■). (b) Dependence of $\Phi_m^{PS\,II}/\Phi_o^{PS\,II}$ on the antenna size for two rate constants for antenna losses calculated by Eq. 5d. Experimental values for pea thylakoids (●) and for *Mantoniella* (■). The theoretical curves were calculated using $k_o^{int} = (0.00179\ ns)^{-1}$ and $k_c^{int} = (0.0191\ ns)^{-1}$ with $k_f = (3.3\ ns)^{-1}$ (solid line) and $k_f = (1.75\ ns)^{-1}$ (dotted line). An antenna size of $N_a = 172$ for pea and $N_a = 287$ in the case of *Mantoniella* was used.

fluorescence induction measurements ($N_a^{PS\ II\alpha}$) and the Chl a/Chl b ratio from BBYs (= 2.3). The Chl $a+b$/P700 ratio was calculated from the Chl a/P700 (= 425) and the Chl a/Chl b ratio of 3.3 measured for thylakoids. The heterogeneity of PS II was quantified by means of fluorescence induction curves yielding 30% PS II_β with a relative antenna size of $N_\alpha/N_\beta = 2.4$ ($N_{a+b}^{PS\ II\alpha}$ and $N_{a+b}^{PS\ II\beta}$). Thus the ratio of (PS II_α + PS II_β)/PS I is 1.4/1. Introducing this value into the extended Eq. 10 yields $N_{a+b}^{PS\ I} = 268$.

The determined PS II/PS I ratio of about 1.5 in *Mantoniella* is not in agreement with those reported elsewhere [2,45]. Dependent on the method used for the determination of PS II/PS I the ratios were 3.68 (P680/P700) or 2.74 (Q_B/P700) for cells grown under low light conditions. There is also a discrepancy concerning the ratio of Chl/P700 which was estimated by Wilhelm et al. [2] to be 1611, whereas it is 1085 in our measurements. Whether the reported differences in the PS II/PS I ratio are due to the different methods used for the estimation or to different culturing conditions remains open.

The methods applied here to determine the antenna sizes of PS I and PS II as well as their stoichiometric ratio from *Mantoniella* thylakoids seems reliable, since for pea thylakoids the same methods resulted in a total PS II antenna size of $N_{a+b} \approx 245$ ($N_a \approx 172 \pm 11$) and a stoichiometric ratio of (PS II_α + PS II_β)/PS I = 1.4/1 which are in close agreement with reported data [46–50].

Determination of k_f. Assuming the same RCs being present in *Mantoniella* and pea thylakoids one can correlate normalized fluorescence yields F_o, F_m, and F_m/F_o-ratios of different organisms with each other by means of the intrinsic rate constants, k_o^{int} and k_c^{int} (Eqs. 4 and 5). Such a comparison of the data from *Mantoniella* with those of pea thylakoids represents an essential constraint to determine the rate constant for antenna losses, k_f.

For the comparison one needs to calculate the fluorescence yields, $\Phi_{m,o}^{PS\ II}$, from the measured fluorescence intensities, F, by means of Eq. 9b. The results of this analysis are summarized in Fig. 5. For pea thylakoids one get $F_o = 1.0$ (normalization), $F_m = 5.85$, and $F_m/F_o = 5.85$ (●) whereas the corresponding data measured for *Mantoniella* are $F_o = 1.48$, $F_m = 4.58$ (the latter two normalized to F_o of peas), and $F_m/F_o = 3.1$ (■).

There are two possibilities to explain the smaller F_m/F_o ratio found for *Mantoniella* compared to peas. It could be due to larger antenna sizes as predicted by Eq. 5d (see Fig. 5b) and/or a stronger quenching in the antenna. To distinguish both possibilities the normalized fluorescence intensities were plotted *vs.* the Chl a antenna size, $N_a = 172$ (pea) and $N_a = 287$ (*Mantoniella*) (Fig. 5). The dependence of the fluorescence yields on the antenna size in the case of pea thylakoids (solid lines) was calculated according to Eqs. 5 assuming $k_f = (3.3\ ns)^{-1}$ which is known from fluorescence lifetime measurements for the isolated LHC II [51,52] and also from fluorescence decay analysis for pea thylakoids. The values of $k_o^{int} = (0.00179\ ns)^{-1}$ and $k_c^{int} = (0.0191\ ns)^{-1}$ resulted from our time resolved fluorescence measurements on pea thylakoids. Both intrinsic rate constants are comparable to those calculated by Roelofs et al. [41] for PS II_α from pea thylakoids [41] ($k_c^{int} = (0.0029\ ns)^{-1}$ and $k_o^{int} = (0.0191\ ns)^{-1}$). The small differences of the intrinsic rate constant of open RCs is consistent with the higher F_m/F_o ratio found for our pea thylakoids.

The data points of pea thylakoids (●) due to quantitative fluorescence intensity measurements match well the theoretical curves derived from the rate constants of the time resolved fluorescence measurements. The corresponding data points of *Mantoniella* (■) lie obviously not on the theoretical curves belonging to pea thylakoids (solid lines).

However, assuming the same intrinsic rate constants as for pea thylakoids and taking a higher rate constant for antenna losses of $k_f = (1.75\ ns)^{-1}$ the *Mantoniella* data can be brought to match the predictions from the exciton-radical pair equilibrium theory (Fig. 5a and b; dotted lines). The faster antenna decay in *Mantoniella* compared to peas, $k_f = (1.75\ ns)^{-1}$ versus $k_f = (3.3\ ns)^{-1}$, may be taken as an indication for a non-negligible transfer of excitons from PS II towards PS I, i.e., PS I-quenching.

One might suspect that the neglect of any PS II heterogeneity renders the foregoing treatment speculative. However, for two reasons this is not the case. First, the description of the fluorescence induction curves obtained from *Mantoniella* thylakoids requires only one population of PS II centers (Fig. 3). Second, the α, β-heterogeneity present in pea thylakoids delivers only a negligible correction as shown by the following calculation. According to Roelofs et al. [41] the fluorescence yields of open and closed RCs are not equal for PS II_α and PS II_β. The published data yield ratios of $\Phi_o^{PS\ II\beta}/\Phi_o^{PS\ II\alpha} = 1.40$ and $\Phi_c^{PS\ II\beta}/\Phi_c^{PS\ II\alpha} = 1.46$. Our pea thylakoids showed 30% PS II_β centers with a relative antenna size of $N_\alpha/N_\beta = 2.4$ as deduced from fluorescence induction measurements (data not shown). With these values one can calculate by means of Eq. 9b the fluorescence yields of pure PS II_α in relation to PS II_α + PS II_β (data in Fig. 5(●)). The F_o from a homogeneous PS II_α pea system is by only 5.5% smaller in comparison to that due to both systems, PS II_α and PS II_β. Analogously, the F_m is by 6.5% smaller.

Fits of fluorescence induction curves. In the framework of the theory developed in Ref. [30] with the adaption given in Section 2, one needs three parameters, F_m/F_o, $\Phi_p(1)$, and J, to define completely a fluorescence induction curve of a homogeneous system. However, in practice more phases are needed to obtain good fits. In the case of our pea thylakoids the consideration of β-centers improved the fit quality by more than a factor of 5 compared to an analysis with α-centers only. The corresponding improvement of the analysis of the fluorescence induction curves from *Mantoniella* amounts to 1.2 (Fig. 3). There-

fore, the contribution of this sort of β-centers in *Mantoniella* is negligible. Assuming no PS II heterogeneity, the best fit of *Mantoniella* yielded $J = 0.89$ (Fig. 3a). Together with the rate constants for losses in the antenna and at open and closed RCs quoted above (which yield also F_m/F_o and $\Phi_p(1)$) one can calculate by means of Eq. 3 the inter-unit exciton exchange rate constant to be $k_{con} = (0.52\ \text{ns})^{-1}$.

In another attempt to fit the fluorescence induction curve we applied the domain theory of Den Hollander et al. [32] for the dimer case (domain size = 2), to check if there is evidence of a dimeric organization of PS II units [22–27]. The poor quality of this fit (Fig. 3d) does not support the **dimer model** (Fig. 1c). For the same reason also the **separated units model** (Fig. 1b) can be excluded for the organization of the PS II units. In summary, the PS II organization in the thylakoid membrane of *Mantoniella* is best described by the **connected units model** composed of α-centers only. It thus appears that β-centers might be specific to the grana/stroma differentiation in higher plants and some green algae as suggested before [28].

PSU organization. The connected units model gives information only about the inter-unit transfer between PS II units. But there is still the question concerning the arrangement and excitonic contact between the both photosystems, PS II and PS I, in the thylakoid membrane of *Mantoniella*.

The exciton decay in PS II proper was described by the rate constants, $k_{a,c}$ and k_f. If an exciton migrates from a PS II unit to a PS I unit it may be included in k_f of PS II since the transfer can be approximated by a virtually irreversible step ($k_f^{PS\,I} >> k_a^{PS\,II} + k_f$).

A rate constant for the exciton transfer from PS II to PS I in *Mantoniella* can be estimated in the following way. If we assume that the LHC_{a+b+c} of *Mantoniella* is also characterized by $k_f^{LHC} = (3.3\ \text{ns})^{-1}$ an effective rate constant for the exciton transfer of $k_{con}^{eff}(\text{PS II} \rightarrow \text{PS I}) = (3.73\ \text{ns})^{-1}$ can be calculated from $k_f = (1.75\ \text{ns})^{-1} = k_{con}^{eff} + k_f^{LHC}$. Taking the PS II/PS I ratio into account a rate constant $k_{con}(\text{PS II} \rightarrow \text{PS I}) = (1.53\ \text{ns})^{-1}$ for the exciton transfer from PS II to PS I follows from $k_{con}(PSII \rightarrow PSI) = \left(k_{con}^{eff}(PSII \rightarrow PSI) / \frac{PSI}{PSI + PSII} \right)$. On the one hand, this means that some excitonic separation of both photosystems, PS I and PS II, is given without structural differentiation of the membrane system into grana and stroma regions. The separation between PS I and PS II in *Mantoniella* obviously suffices to allow for different antenna sizes of both photosystems. On the other hand, the separation is not as good as in the photosynthetic apparatus of higher plants. As a consequence, the maximal photochemical yield is lower (75% in the case of *Mantoniella* compared to about 90% in pea thylakoids).

One may argue that the increased k_f of *Mantoniella* has other reasons than the PS I quenching alone, e.g., quenching by the oxidized plastoquinones or by carotenoids, that may be involved in non-photochemical quenching. However, if this case would be considered the calculated separation between PS I and PS II would increase. In conclusion, our estimation of $k_{con}(\text{PS II} \rightarrow \text{PS I}) = (1.53\ \text{ns})^{-1}$ represents an upper limit of the connectivity between PS I and PS II in *Mantoniella* thylakoids.

Although a **pure dimer model** yields a worse fit compared to the **connected units model** we cannot excluded that the PS II units in *Mantoniella* are arranged as dimers. There are two things that make a more sophisticated analysis difficult: (1) The dimers may not be perfectly connected and (2) perfectly connected dimers may show some degree of connectivity to neighboring dimer units. Due to these uncertainties the question of the existence of PS II dimers in *Mantoniella* remains open.

Acknowledgements

B.H and H.-W.T. thank Prof. W. Junge for laboratory facilities. The financial support of the Deutsche Forschungsgemeinschaft (SFB 171-A1) is acknowledged.

References

[1] Krämer, P., Wilhelm, C., Wild, A., Mörschel, E. and Rhiel, E. (1988) Protoplasma 147, 170–177.
[2] Wilhelm, C., Krämer, P. and Lenartz-Weiler, I. (1989) Photosynth. Res. 20, 221–233.
[3] Bennett, J. (1991) Annu. Rev. Plant Physiol. Plant Mol. Biol. 42, 281–311.
[4] Allen, J.F. (1992) Biochim. Biophys. Acta 1098, 275–335.
[5] Rhiel, E. and Mörschel, E. (1993) Mol. Gen. Genet. 240, 403–413.
[6] Schmitt, A., Frank, G., James, P., Staudenmann, W., Zuber, H. and Wilhelm, C. (1994) Photosynth. Res. 40, 269–277.
[7] Mullet, J.E. (1983) J. Biol. Chem. 258, 9941–9948.
[8] Fawley, M.W., Stewart, K.D. and Mattox, K.R. (1986) J. Mol. Evol. 23, 168–176.
[9] Wilhelm, C. (1990) Plant Physiol. Biochem. 28, 293–306.
[10] Rhiel, E., Lange, W. and Mörschel, E. (1993) Biochim. Biophys. Acta 1143, 163–172.
[11] Schmitt, A., Herold, A., Welte, C., Wild, A. and Wilhelm, C. (1993) Photochem. Photobiol. 57, 132–138.
[12] Brown, J.S. (1985) Biochim. Biophys. Acta 807, 143–146.
[13] Govindjee, Cederstrand, C. and Rabinowitch, E. (1961) Science 134, 391–392.
[14] Brown, J.S. (1988) J. Phycol. 24, 96–102.
[15] Chrystal, J. and Larkum, A.W.D. (1988) Biochim. Biophys. Acta 932, 189–194.
[16] Berkaloff, C., Caron, L. and Rousseau, B. (1990) Photosynth. Res. 23, 181–193.
[17] Trissl, H.-W. (1993) Photosynth. Res. 35, 247–263.
[18] Trissl, H.-W. and Wilhelm, C. (1993) Trends Biochem. Sci. 18, 415–419.
[19] Glazer, A.N. (1984) Biochim. Biophys. Acta 768, 29–51.
[20] MacColl, R. and Guard-Friar, D. (1987) Anonymous Phycobili proteins. Boca Raton, Florida, CRC Press.
[21] Wilhelm, C. and Duval, J.-C. (1990) Biochim. Biophys. Acta 1016, 197–202.

[22] Boekema, E.J., Hankamer, B., Bald, D., Kruip, J., Nield, J., Boonstra, A.F., Barber, J. and Rögner, M. (1995) Proc. Natl. Acad. Sci. USA 92, 175–179.
[23] Seibert, M., DeWit, M. and Staehelin, L.A. (1987) J. Cell Biol. 105, 2257–2265.
[24] Peter, G.F. and Thornber, J.P. (1991) Plant Cell Physiol. 32, 1237–1250.
[25] Lyon, M.K., Marr, K.M. and Furcinitti, P.S. (1993) J. Struct. Biol. 110, 133–140.
[26] Santini, C., Tidu, V., Tognon, G., Magaldi, A.G. and Bassi, R. (1994) Eur. J. Biochem. 221, 307–315.
[27] Rögner, M., Boekema, E.J. and Barber, J. (1995) Trends Biochem. Sci.
[28] Anderson, J.M. and Melis, A. (1983) Proc. Natl. Acad. Sci. USA 80, 745–749.
[29] Lavergne, J. and Briantais, J.-M. (in press) in Oxygenic Photosynthesis: The Light Reactions, Series Advances in Photosynthesis, (Ort, D.R. and Yocum, C.F. ed.), Kluwer Academic Publishers, Dordrecht.
[30] Lavergne, J. and Trissl, H.-W. (1995) Biophys. J. 65, 2474–2492.
[31] Laible, P.D., Zipfel, W. and Owens, T.G. (1994) Biophys. J. 66, 844–860.
[32] Den Hollander, W.T.F., Bakker, J.G.C. and Van Grondelle, R. (1983) Biochim. Biophys. Acta 725, 492–507.
[33] Trissl, H.-W. and Lavergne, J. (1995) Austr. J. Plant Physiol. 22, 183–193.
[34] Müller, D. (1962) Bot. Mar. 314, 140–155.
[35] Porra, R.J., Thompson, W.A. and Kriedemann, P.E. (1989) Biochim. Biophys. Acta 975, 384–394.
[36] Hiyama, T. and Ke, B. (1972) Biochim. Biophys. Acta 267, 160–171.
[37] Trissl, H.-W. and Wulf, K. (1995) Biospectroscopy 1, 71–82.
[38] Wulf, K. and Trissl, H.-W. (1995) Biospectroscopy 1, 55–69.
[39] Schatz, G.H., Brock, H. and Holzwarth, A.R. (1988) Biophys. J. 54, 397–405.
[40] Leibl, W., Breton, J., Deprez, J. and Trissl, H.-W. (1989) Photosynth. Res. 22, 257–275.
[41] Roelofs, T.A., Lee, C.-H. and Holzwarth, A.R. (1992) Biophys. J. 61, 1147–1163.
[42] Lavergne, J. and Etienne, A.-L. (1980) Biochim. Biophys. Acta 593, 136–148.
[43] Malkin, S., Armond, P.A., Mooney, H.A. and Fork, D.C. (1981) Plant Physiol. 67, 570–579.
[44] Malkin, S. and Fork, D.C. (1981) Plant Physiol. 67, 580–583.
[45] Wilhelm, C., Krämer, P. and Lenartz-Weiler, I. (1990) Crypt. Bot. 1, 355–359.
[46] Mauzerall, D. and Greenbaum, N.L. (1989) Biochim. Biophys. Acta 974, 119–140.
[47] Melis, A. (1991) Biochim. Biophys. Acta 1058, 87–106.
[48] Harrison, M.A. and Melis, A. (1992) Plant Cell Physiol. 33, 627–637.
[49] Kim, J.H., Glick, R.E. and Melis, A. (1993) Plant Physiol. 102, 181–190.
[50] Jansson, S. (1994) Biochim. Biophys. Acta 1184, 1–19.
[51] Eads, D.D., Webb, S.P., Owens, T.G., Mets, L.J., Alberte, R.S. and Fleming, G.R. (1987) in Progress in Photosynthesis Research, (Biggins, J. ed.), Vol. III, pp. 135–138, Martinus Nijhoff Publishers, Dordrecht.
[52] Ide, J.P., Klug, D.R., Kühlbrandt, W., Giorgi, L.B. and Porter, G. (1987) Biochim. Biophys. Acta 893, 349–364.